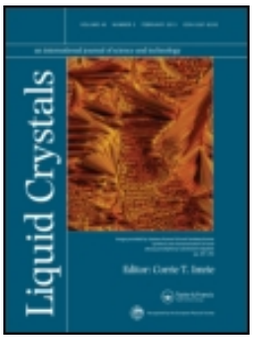

Liquid Crystals

ISSN: 0267-8292 (Print) 1366-5855 (Online) Journal homepage: https://www.tandfonline.com/loi/tlct20

Effect of alkyl chain length of alcohols on nematic uniaxial-to-biaxial phase transitions in a potassium laurate/alcohol/K_2SO_4/water lyotropic mixture

Erol Akpinar , Dennys Reis & Antonio Martins Figueiredo Neto

To cite this article: Erol Akpinar , Dennys Reis & Antonio Martins Figueiredo Neto (2012) Effect of alkyl chain length of alcohols on nematic uniaxial-to-biaxial phase transitions in a potassium laurate/alcohol/K_2SO_4/water lyotropic mixture, Liquid Crystals, 39:7, 881-888, DOI: 10.1080/02678292.2012.686637

To link to this article: https://doi.org/10.1080/02678292.2012.686637

Published online: 14 May 2012.

Liquid Crystals,
Vol. 39, No. 7, July 2012, 881–888

Taylor & Francis
Taylor & Francis Group

Effect of alkyl chain length of alcohols on nematic uniaxial-to-biaxial phase transitions in a potassium laurate/alcohol/K_2SO_4/water lyotropic mixture

Erol Akpinar[a], Dennys Reis[b] and Antonio Martins Figueiredo Neto[b]*

[a]*Abant Izzet Baysal University, Arts and Sciences Faculty, Department of Chemistry, Bolu, Turkey;* [b]*Universidade de São Paulo, Instituto de Física, São Paulo, SP, Brazil*

(*Received 13 March 2012; final version received 16 April 2012*)

Lyotropic liquid crystalline quaternary mixtures of potassium laurate (KL), potassium sulphate (K_2SO_4)/alcohol (*n*-OH)/water, with the alcohols having different numbers of carbon atoms in the alkyl chain (*n*), from 1-octanol to 1-hexadecanol, were investigated by optical techniques (optical microscopy and laser conoscopy). The biaxial nematic phase domain is present in a window of values of $n = n_{KL} \pm 2$, where $n_{KL} = 11$ is the number of carbon atoms in the alkyl chain of KL. The biaxial phase domain became smaller and the uniaxial-to-biaxial phase transition temperatures shifted to relatively higher temperatures upon going from 1-nonanol to 1-tridecanol. Moreover, compared with other lyotropic mixtures these new mixtures present high birefringence values, which we expect to be related to the micellar shape anisotropy. Our results are interpreted assuming that alcohol molecules tend to segregate in the micelles in a way that depends on the relative value of *n* with respect to n_{KL}. The larger the value of *n*, the more alcohol molecules tend to be located in the curved parts of the micelle, favoring the uniaxial nematic calamitic phase with respect to the biaxial and uniaxial discotic nematic phases.

Keywords: lyotropic; birefringence; conoscopy; molecular segregation

1. Introduction

After the experimental realization of the biaxial nematic phase (N_B) in a lyotropic mixture of potassium laurate (KL)/1-decanol (DeOH)/water by Yu and Saupe in 1980 [1], during the last three decades some research groups have reported on new mixtures presenting the N_B phase [2–9]. These studies were useful in understanding the physical–chemical characteristics of this remarkable phase, its chemical stability and the symmetry of the micelles in these mixtures. For instance, some authors proposed that the biaxial phase reflects the co-existence of two uniaxial nematic discotic N_D and calamitic N_C phases. From the nanoscopic point of view, this idea leads to the so-called 'mixtures of cylindrical-like and disc-like micelles' (MCD) model [10]. This type of model had many problems [11–13], and a different approach was proposed by Neto *et al.* [14] and Galerne *et al.* [15]. They proposed the intrinsically biaxial micelles (IBM) model, which is based on the different orientational fluctuations of the same type of micelle in the three nematic phases.

One of the most easy and reliable experimental methods to investigate uniaxial-to-biaxial phase transitions is laser conoscopy [16, 17]. This technique is particularly useful in the case of materials with small birefringence ($\sim 10^{-3}$), where thick samples are needed to allow an accurate measurement of birefringences.

Macroscopically, the N_B phase has orthorhombic symmetry and, consequently, three different indices of refraction, along the three orthogonal symmetry axes, each one of these axes of order two [18]. As a consequence, two birefringences are present, defined as the differences between two of the principal indices of refraction. The nematic phases are characterized by an order parameter that is a second-rank, symmetric and traceless tensor. Practically, the optical dielectric tensor may be chosen as the order parameter and it can be calculated from the measurements of the birefringences [17]. Moreover, the temperature dependences of the birefringences are very useful for the determination of the phase transition temperatures between the uniaxial-to-biaxial nematics, and also to build up phase diagrams.

On comparing the phase diagrams of lyotropic mixtures published in the literature to date, they give, in general, similar biaxial phase properties in terms of the temperature range of the biaxial phase and maximum value of the nematic birefringence ($\sim 2 \times 10^{-3}$) [19]. Assuming the IBM model, it is expected that the higher the birefringence value, the more anisometric the micelles should be. An interesting result encountered so far is that in all the lyotropic mixtures presenting the N_B phase, there is always a surfactant and a co-surfactant [18]. Mixtures with only one surfactant

*Corresponding author. Email: afigueiredo@if.usp.br

ISSN 0267-8292 print/ISSN 1366-5855 online

http://dx.doi.org/10.1080/02678292.2012.686637
http://www.tandfonline.com

were shown to present only one of the uniaxial nematic phases, the N_C or the N_D phase. Alcohol is commonly employed [1, 3] as a co-surfactant; however, mixtures with soap and a detergent [5] also presented the N_B phase.

Let us now concentrate our attention on the alcohol molecules present in lyotropic mixtures. Consider a micellar system composed of an amphiphilic compound, water and salt. In this system three different regions may be identified [20]: the first is the aqueous region (intermicellar region) that contains dissolved counterions of the surfactants, a small amount of free amphiphiles and the dissociated salt ions; the second region (interfacial region or palisade layer [21]) consists of the headgroups of the surfactants, some amount of counterions and water; the third region (hydrophobic core) is composed of the surfactant alkyl chains. When alcohol molecules are added to this mixture they may be located in these regions, depending on their characteristics. Short-chain alcohol molecules, such as ethanol, are completely miscible with water and are mostly found in the intermicellar and palisade regions. However, they cannot efficiently penetrate into the micellar core. Then, the mole fraction of ethanol incorporated in the micelle should be smaller than that in the intermicellar. The mole fraction of alcohol molecules incorporated in the micelles (X_A) may be different from the mole fraction in the intermicellar region (X_B). The ratio between these two quantities is known as the partition coefficient of the alcohol, $K_p = X_A/X_B$ [22, 23]. The bigger the number of carbon atoms in the alkyl chain of the alcohol molecule, the bigger K_p [22–26]. Since short-chain alcohols have higher solubility in water than long-chain alcohols, short-chain alcohols have smaller K_p values than longer-chain alcohols. In other words, while short-chain alcohols preferentially exist in the intermicellar region, long-chain alcohols are mainly incorporated into the micelles [21, 27]. For example, the K_p value of hexanol is 758, approximately 18 times that of butanol ($K_p = 42.2$) in aqueous micellar solutions of lithium dodecylsulfate [28]. In lipid membrane/buffer systems, the partition coefficients (defined here as the ratio of molar concentration of alcohol in the lipid bilayer and in the buffer – or water layer) of decanol, undecanol, dodecanol, tridecanol, tetradecanol and pentadecanol are 3.9×10^3, 1.7×10^4, 6.9×10^4, 3.1×10^5, 1.4×10^6 and 5.6×10^6, respectively [29]. This means that, in terms of the molar concentrations or number of alcohol molecules in the bilayer (or in the hydrophobic core), pentadecanol incorporates many more molecules than decanol.

To the best of our knowledge, in the literature there is no systematic investigation of the effect of the number of carbons in the alkyl chain of the alcohol molecules (n) on the topology of lyotropic mixtures presenting the biaxial nematic phase. In this study we investigate the phase sequence of 10 new lyotropic mixtures of KL/K_2SO_4/1-nOH/water, with $n = 6$ and $8 \leq n \leq 16$, determining the location of the N_B phase. Optical microscopy and laser conoscopy experimental techniques are used to characterize the phases.

2. Experimental details

Sample preparation, in particular the homogenisation procedure, has been discussed elsewhere [18]. This aspect is extremely important to obtain reproducible results. To improve the orientation of the samples in the magnetic field, a small amount ($\sim$1 μL ferrofluid per 1 g of mixture) of water-based ferrofluid was added to the mixtures [18]. For observation of the textures under a light polarised optical microscope, each sample was transferred into a 0.2 mm-thick flat-glass microslide.

Besides the texture characterization, the nematic sample's birefringences were measured by using laser conoscopy [17]. The laboratory frame axes were defined as follows: the horizontal plane is defined by the two orthogonal axes 1 and 2; the magnetic field is aligned along the axis 1; axis 3 is vertical and parallel to the laser beam propagation direction. Two main optical birefringences, $\Delta n = n_2 - n_1$ and $\delta n = n_3 - n_2$, were measured as a function of temperature. Mixtures were put in the sample cell made of two circular optical glasses and a glass o-ring, leaving a liquid crystalline film 1.0 mm thick. A sample's birefringences were measured as a function of temperature (T). The experimental set-up has a HeNe laser ($\lambda = 632.8$ nm) and a Neocera LTC-21 temperature controller, with accuracy of 0.001°C. A Walker Sci. electromagnet provides the static magnetic field $\left(|\vec{H}| = 2.04\,\mathrm{kG}\right)$ used to orient the sample.

To obtain a well-aligned N_D phase, the samples were kept at a fixed temperature for about 30–60 min, after which the temperature was slowly varied step by step. At each new temperature the sample was left at rest for at least 10 min in order to achieve thermal equilibrium. From time to time, in the N_D (N_B) phase, the sample was turned through an angle of about $\pm\pi/2$ ($\pm\pi/6$) around axis 3 to improve the sample orientation.

Mixtures are named according to the number of carbon atoms in the alkyl chain, e.g. n_{10} corresponds

Table 1. Molar fractions (X) of each components in the lyotropic mixtures investigated. ΔT_B is the temperature range of the biaxial nematic domain.

Mixture	Alcohol	X_{KL}	$X_{K_2SO_4}$	$X_{alcohol}$	X_{H_2O}	Nematic phase type	$\Delta T_{N_B}/^\circ C$
n_6	HeOH	0.0383	0.0060	0.0114	0.9443	—	—
n_8	OcOH	0.0382	0.0060	0.0114	0.9443	N_D	—
n_9	NonOH	0.0383	0.0060	0.0114	0.9443	N_B,N_D	> 6
n_{10}	DeOH	0.0383	0.0060	0.0114	0.9443	N_C,N_B,N_D	∼7.80
n_{11}	UnDeOH	0.0383	0.0060	0.0114	0.9443	N_C,N_B,N_D	∼5.55
n_{12}	DDeOH	0.0383	0.0060	0.0114	0.9443	N_C,N_B,N_D	∼3.30
n_{13}	TDeOH	0.0383	0.0060	0.0114	0.9443	N_C,N_B,N_D	∼1.70
n_{14}	TeDeOH	0.0382	0.0060	0.0114	0.9443	N_C	—
n_{15}	PDeOH	0.0382	0.0060	0.0114	0.9443	N_C	—
n_{16}	HDeOH	0.0383	0.0060	0.0114	0.9443	N_C	—

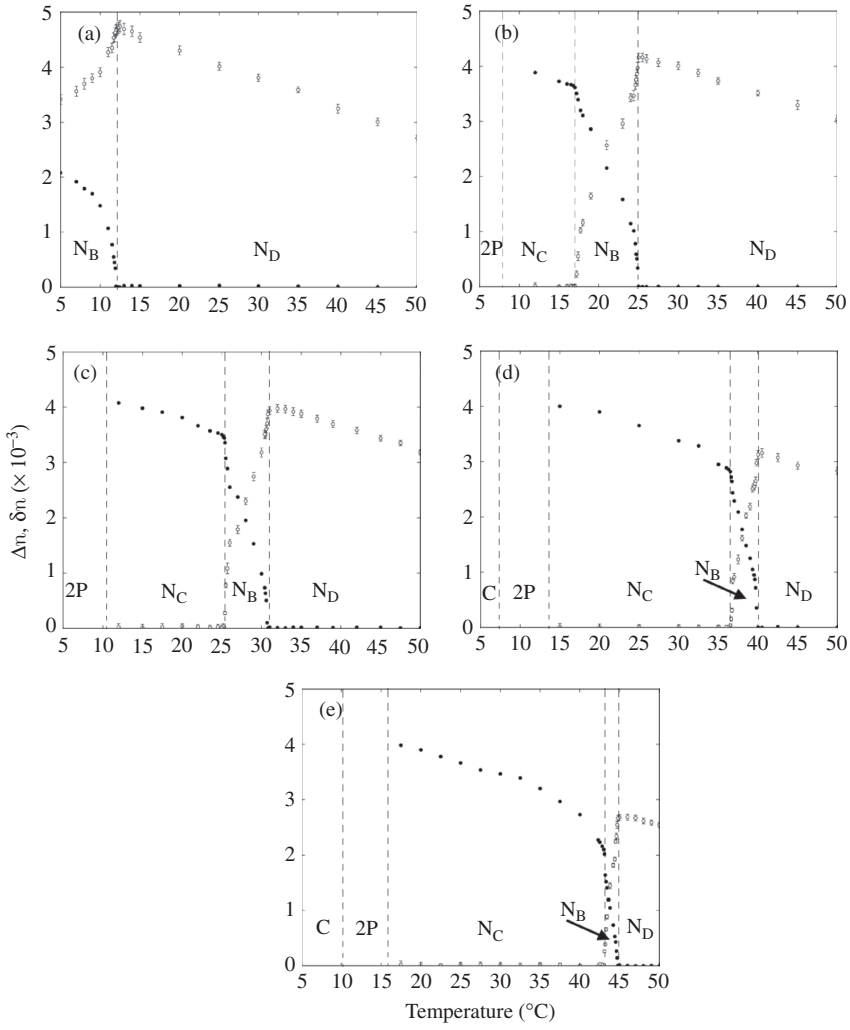

Figure 1. Birefringences of the mixtures of (a) n_9, (b) n_{10}, (c) n_{11}, (d) n_{12}, and (e) n_{13}, as a function of the temperature. $\Delta n = n_2 - n_1$ (•) and $\delta n = n_3 - n_2$ (○). The labels 2P and C stand for the two-phase and crystalline regions, respectively.

to the KL/K_2SO_4/1-decanol/water mixture, n_{16} corresponds to the KL/K_2SO_4/1-hexadecanol/water, and so on. Table 1 presents the molar fractions of the different mixture components, types of identified nematic phases and the temperature range of the biaxial nematic phase, when present.

3. Result and discussion

The textures of the mixtures were identified under a polarising light microscope. In general, the textures observed were similar to those from typical nematic lyotropic mesophases [18]. The different nematic phases and phase transition temperatures were obtained from birefringence measurements and texture identification. Inspection of the textures under crossed polarisers helps us to identify the different nematic phases; in particular, it is easy to differentiate the N_D phase from the N_C and N_B phases [18]. This can be done by applying a magnetic field in the plane of the flat-glass microslide (sample holder), perpendicular to the direction of light propagation. In this condition a homeotropic texture is stabilized in the N_D phase. If inversion walls appear, the nematic phase is N_C or N_B. To identify the phase beyond doubt, the conoscopy experiment is necessary.

Since the mixtures from n_9 until n_{13} show the N_D phase at higher temperatures, well-oriented N_D phases were obtained by applying a static magnetic field to the sample; then the optical birefringences of each nematic phase as a function of temperature were measured, starting from the N_D phase, upon cooling. The experimental results of Δn and δn as a function of T, from these mixtures, keeping constant the molar fractions of all constituents in all mixtures (see Table 1), are shown in Figure 1. It is interesting to note that upon going from n_9 to n_{13}, the uniaxial-to-biaxial phase transitions shift to higher temperatures and the biaxial nematic domain gets smaller.

The phase diagram depicted in Figure 2 was constructed by plotting the different phases identified at temperature (T) versus the number of the carbon atoms (n) in the alkyl chain of the alcohols. Special care must be taken in the conclusions drawn from the plot shown in Figure 2, because the temperature assumes continuous values (intensive thermodynamic variable), and assumes n only a discrete set of positive values. The data were obtained from both laser conoscopy and optical polarising microscopy. The existence of the three nematic phases is restricted to the range of values of n from $n = 9$ to $n = 13$. A mixture with 1-hexanol was also prepared; however, this mixture was highly viscous and its homogeneity was hardly achieved. Visual inspection seems to indicate

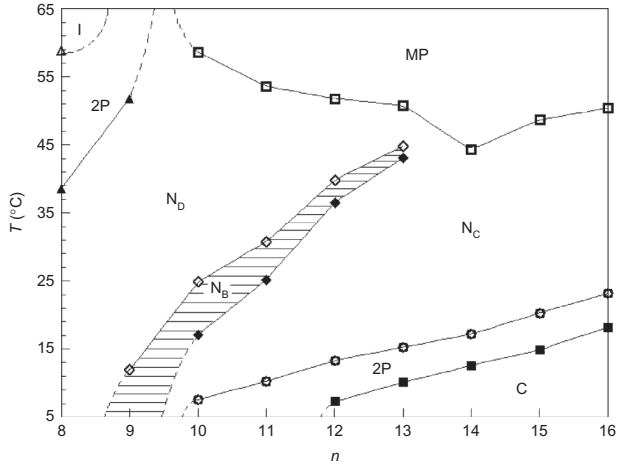

Figure 2. Phase diagram of the lyotropic mixtures: temperature versus the number of carbon atoms in the alkyl chain of the alcohols. I, 2P, MP and C stand for an isotropic phase, two-phase region, multi-phase region and crystalline phase, respectively. Solid and dashed lines are only guides. The hatched region depicts the biaxial nematic phase domain.

the presence of a gel phase throughout the temperature range investigated.

The optical birefringences in these new quaternary lyotropic mixtures are higher when compared with those from the usual ternary KL/DeOH/water mixture. In particular, in the N_D phase of our quaternary mixtures with nonanol, decanol and undecanol, birefringence reaches values greater than 4×10^{-3}, almost two times the maximum value encountered in the KL/DeOH/water system [19]. These high birefringence values are not due to the ferrofluid doping,

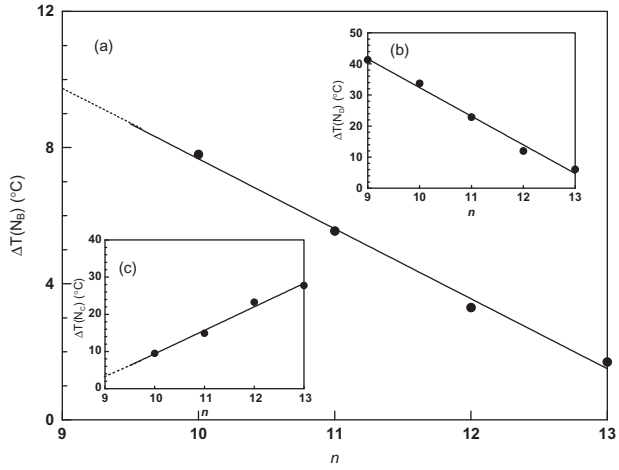

Figure 3. Temperature intervals of the N_B (a), N_D (b) and N_C (c) nematic phases of the different quaternary mixtures, where n represents the number of carbons on the alkyl chains of the alcohols. Solid lines are linear fits.

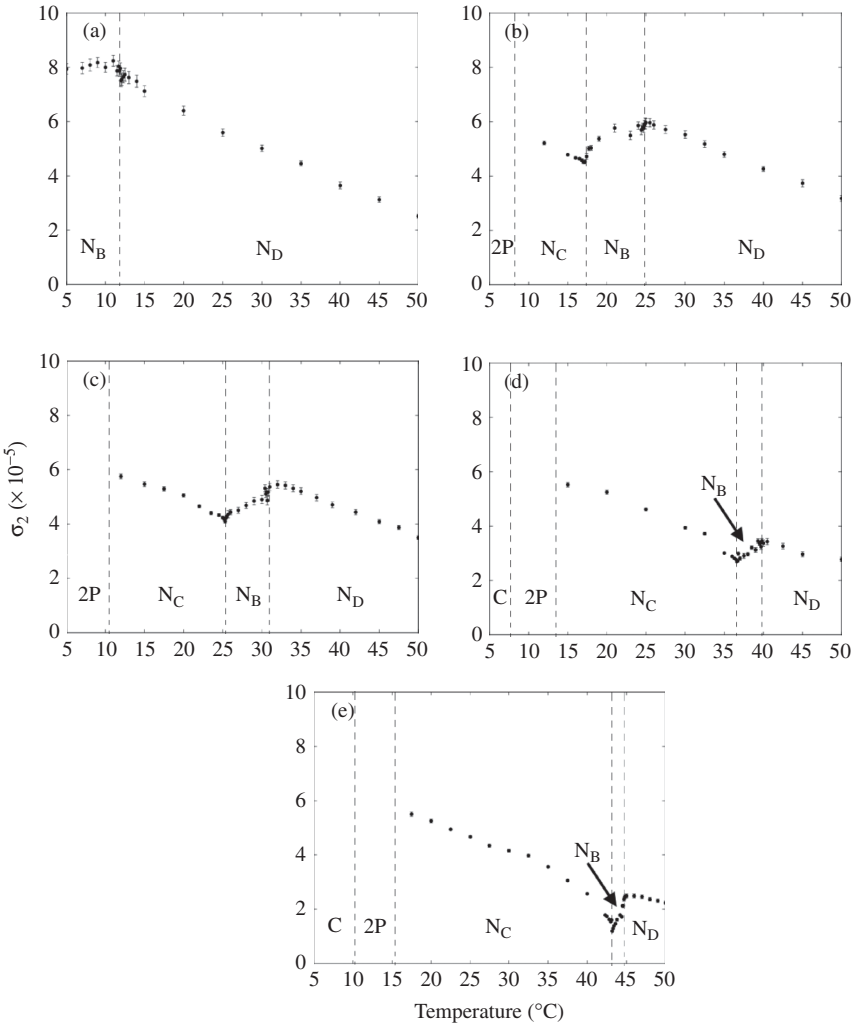

Figure 4. Order-parameter invariant σ_2 versus T: (a) 1-nonanol, (b) 1-decanol, (c) 1-undecanol, (d) 1-dodecanol and (e) 1-tridecanol mixtures. 2P and C are the two-phase and crystalline phase regions, respectively.

which we checked by measuring the birefringences of (doped) sample with $n = 8$ in the isotropic phase: within our experimental accuracy $\Delta n = \delta n = 0$. Upon going from 1-decanol to 1-tridecanol, the N_B and N_D domains got smaller and the N_C domain increased (Figure 3).

The nematic phases of lyotropic liquid crystals are characterized by a second-rank, traceless, symmetric-tensor order parameter [30, 31]. The optical dielectric tensor, $\overleftrightarrow{\varepsilon}$, which has the same symmetry of the phases, may be chosen as the order parameter [32]. The symmetric invariants of the tensor order parameter, σ_1, σ_2 and σ_3 are calculated from the birefringence measurements [17]. The first invariant σ_1 is simply the trace of the tensor which, in this case, is equal to zero. In the uniaxial phases the invariant σ_3 is related to σ_2 by $\sigma_3 = \pm\sigma_2^{3/2}$ [17]. The signs + (–) refer to the N_D (N_C) phase. In the biaxial phase $-\sigma_2^{3/2} < \sigma_3 < \sigma_2^{3/2}$. Figures 4 and 5 show the dependences of σ_2 and σ_3 on temperature of the mixtures presenting the N_B phase, respectively. The mean-field theory predicts that, near the uniaxial-to-biaxial phase transitions, σ_2 and σ_3 depend linearly on T. This behaviour is observed in Figures 4 and 5. Figure 6 shows the σ_3 values plotted against σ_2, and the solid lines represent the σ_3 versus σ_2 theoretical behaviour for the uniaxial nematic phases. The invariants of the order parameter also reach high values.

In our case, all the alcohols used in this study present high partition coefficients K_p [29]. Since they are completely immiscible in water, we should discuss the locations of their head groups, -OH, in the palisade layer and the hydrophobic tails in the micelle core. In the framework of the IBM model [15, 18], the higher the birefringences of the nematic phase, the larger the shape anisotropy of the micelles. Therefore, our new

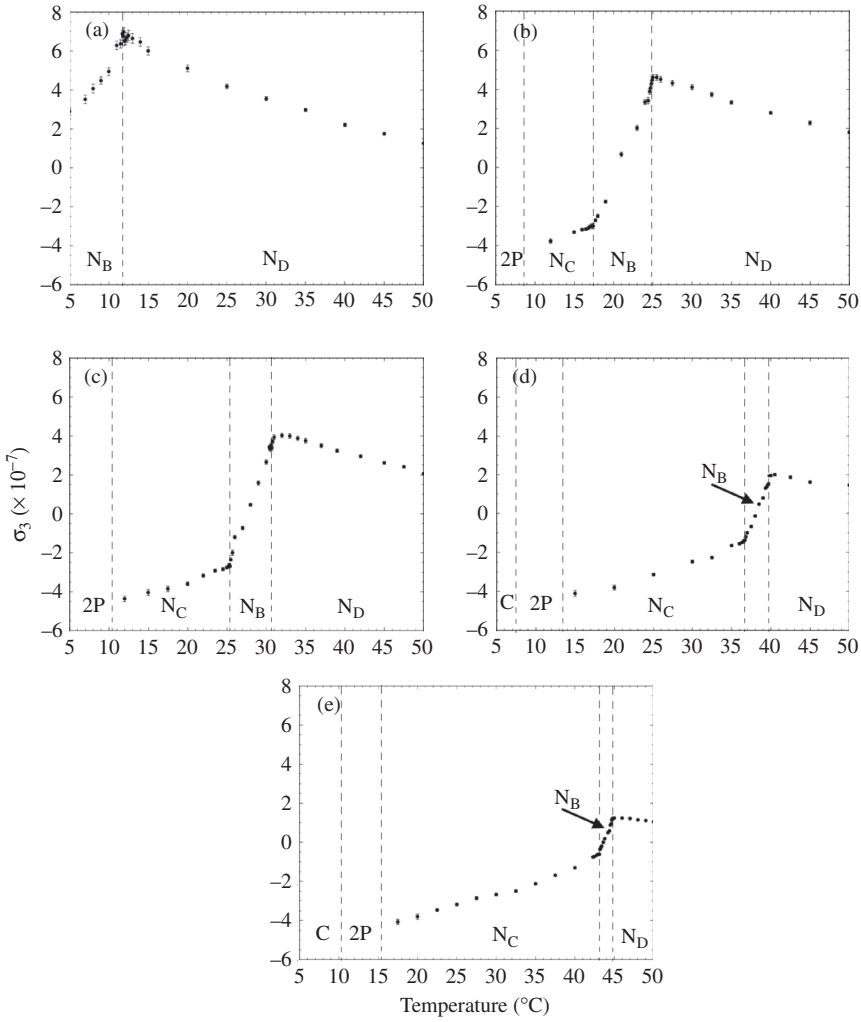

Figure 5. Order parameter invariant σ_3 versus T: (a) 1-nonanol, (b) 1-decanol, (c) 1-undecanol, (d) 1-dodecanol and (e) 1-tridecanol mixtures. 2P and C are the two-phase and crystalline phase regions, respectively.

quaternary mixtures are expected to show more anisometric micelles when compared with those from the usual KL/DeOH/water system, since the maximum values of the birefringences measured in this quaternary mixture lies between 3×10^{-3} and 4×10^{-3} in the nematic temperature range. Let us sketch a micelle as an object of orthorhombic symmetry, as in Figure 7, with typical dimensions A', B' and C'. The axes of the coordinate system fixed in the micelles are α, β and γ, and the laboratory frame axes are 1, 2 and 3.

According to neutron contrast experiments with the lyotropic mixture KL/DeOH/water, alcohol molecules concentrate, mainly, in the flattest surface of the micelle, rather than in its curved borders [33]. This result indicates that there is segregation on the partitions of the surfactant and alcohol molecules in the less curved areas and rims of the micelles. From an experimental point of view, the increase of the relative concentration of alcohol and water in the mixture was shown to enlarge the N_D phase domain [2]. This result may be interpreted as an increase of the dimensions of the micelles in the plane $\alpha - \beta$. This geometry favors the orientational fluctuation that degenerates axis 3, stabilising the N_D phase. In our present experiment the mole fractions of the different compounds are constant in all the mixtures investigated. So, the effect of changing the different nematic phase domain sizes is due to the relative difference between n (number of carbon atoms in the alkyl chain of the different alcohols) and n_{KL} (= 11, number of carbon atoms in the alkyl chain of the surfactant, except that placed at the polar head [34]). The N_B phase appears in a window of $n = n_{KL} \pm 2$. When $n < 11$ our results show the prevalence of the N_D, with respect to other nematic phases. We expect that, in this case, alcohol molecules accumulate preferentially in the largest micellar surfaces, and the micellar dimensions are such that $A' \sim B'$. However, it must be pointed out that the dimensions A' and B' must be different to give rise to the N_B phase observed

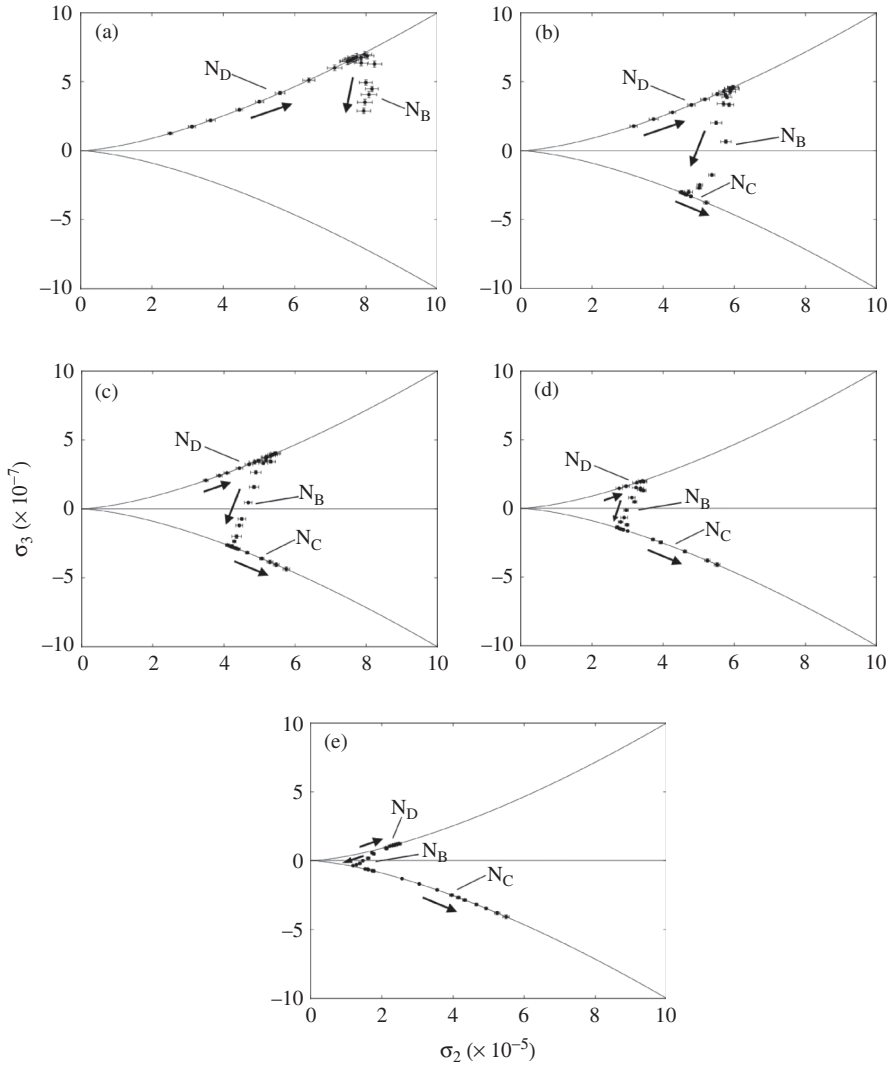

Figure 6. Dependence of invariant σ_3 with respect to σ_2 for the mixtures (a) 1-nonanol, (b) 1-decanol, (c) 1-undecanol, (d) 1-dodecanol and (e) 1-tridecanol, at working temperature range. Solid lines represent the mean-field σ_3 versus σ_2 theoretical behaviour for the uniaxial nematic phases. The arrows indicate the cooling process employed to measure the birefringences, starting from the N_D phase.

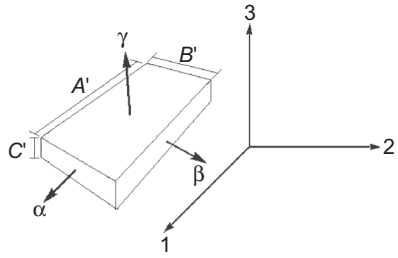

Figure 7. Sketch of the orthorhombic micelle, in the framework of the IBM model. The surfactant amphiphilic bilayer is represented by C'.

in these mixtures. This particular shape anisometry favors the orientational fluctuations that degenerate the axis 3, giving rise to the N_D phase. When $n > 11$, alcohol molecules may accommodate themselves also in the curved parts of the micelle in a larger number. By affinity, it is expected that these molecules tend to concentrate in a particular place in the micelle, increasing the shape anisotropy in the $\alpha - \beta$ plane. When $n > 11$, the presence of long-chain alcohol molecules in the more flat part of the micelle (with bilayer of $C' = 2.6$ nm [15]) becomes more difficult, and the alcohol molecules tend to concentrate in the curved parts of the micelle, increasing still more the shape anisotropy in the $\alpha - \beta$ plane. This behaviour favors the increase of one of the micellar dimensions, let us say *A*' with respect to *B*' in our sketch in Figure 7, and the orientational fluctuation which is favored is the one which degenerates the axis 1, i.e. privileging the N_C phase.

This accumulation of alcohol molecules in the more curved part of the micelle may be interpreted as

a nanosegregation due to the affinity between identical long-chain molecules, giving rise to an increase of one of the micellar dimension (*A*') with respect to the other (*B*'). At this point we define a phenomenological partition coefficient (similar to that discussed in the Introduction section), that takes into account the process of alcohol segregation in the micelle employed here, to interpret our experimental results. Let K_p^m be the ratio of the mole fraction of alcohol molecules in the more curved surfaces to that of the more flat surfaces of the micelle. The higher the K_p^m value, the more alcohol molecules accumulate in the curved parts of the micelle. Our results seem to indicate that an increase in the carbons in the alcohol alkyl chain leads to an increase of K_p^m, since increasing n the N_C phase domain increases at the expense of the N_D and N_B phase domains.

4. Conclusions

We investigated the phase diagram of the quaternary mixture of KL/K_2SO_4/alcohol/water as a function of temperature and number of carbon atoms in the alcohol alkyl chain (n), where three nematic phases are present. We show that the biaxial nematic phase domain exists in a window of values of n varying around the number of carbon atoms of the KL chain, with $n = n_{KL} \pm 2$. The higher the value of n the larger the N_C phase domain, when compared with the N_D and N_B phase domains. Assuming that micelles have an orthorhombic symmetry (IBM model in the nematic phases), our results suggest that the alcohol molecules segregate in different ways, depending on the value of n with respect to n_{KL} : for $n < n_{KL}$ there is a tendency of the alcohol molecules accumulate more in the flattest surface of the micelles, favoring the N_D phase; for $n > n_{KL}$ alcohol molecules tend accommodate preferentially in the curved surfaces of the micelle, favoring the N_C phase. This segregation of the alcohol molecules seems to maintain the orthorhombic symmetry of the micelles, probably due to the fact that similar molecules tend to remain together.

Acknowledgements

We thank The Scientific and Technological Research Council of Turkey (TÜBİTAK), the National Institute of Science and Technology on Complex Fluids (INCT-FCx), CNPq and FAPESP from Brazil for supporting this study.

References

[1] Yu, L.J.; Saupe, A. *Phys. Rev. Lett.* **1980**, *45*, 1000–1003.
[2] Figueiredo Neto, A.M.; Liebert, L.; Galerne, Y. *J. Phys. Chem.* **1985**, *89*, 3737–3739.
[3] Bartolino, R.; Chiaranza, T.; Meuti, M.; Compagnoni, R. *Phys. Rev. A: At., Mol., Opt. Phys.* **1982**, *26*, 1116–1119.
[4] Galerne, Y.; Liebert, L. *Phys. Rev. Lett*. **1985**, *55*, 2449–2451.
[5] Oliveira, E.A.; Liebert, L.; Figueiredo Neto, A.M. *Liq. Cryst.* **1989**, *5*, 1669–1675.
[6] Vasilevskaya, A.S.; Kitaeva, E.L.; Sonin, A.S. *Russ. J. Phys. Chem.* **1990**, *64*, 599–601.
[7] Quist, P.-O. *Liq. Cryst.* **1995**, *18*, 623–629.
[8] Ho, C.C.; Hoetz, R.J.; El-Aasser, M.S. *Langmuir* **1991**, *7*, 630–635.
[9] de Melo Filho, A.A.; Lavarde Jr., A.; Fujiwara, F.Y. *Langmuir* **2003**, *19*, 1127–1132.
[10] Stroobants, A.; Lekkerkerker, H.N.W. *J. Phys. Chem*. **1984**, *88*, 3669–3674.
[11] Palffy-Muhoray, P.; de Bruyn, J.R.; Dunmur, D.A. *J. Chem. Phys*. **1985**, *82*, 5294–5295.
[12] Sharma, S.R.; Palffy-Muhoray, P.; Bergen, B.; Dunmur, D.A. *Phys. Rev. A: At., Mol., Opt. Phys.* **1985**, *32*, 3752–3755.
[13] van der Kooij, F.M.; Lekkerkerker, H.N.W. *Langmuir* **2000**, *16*, 10144–10149.
[14] Figueiredo Neto, A.M.; Galerne, Y.; Levelut, A.M.; Liebert L. *J. Phys. (Paris) Lett*. **1985**, *46*, L-409–505.
[15] Galerne, Y.; Figueiredo Neto, A.M.; Liebert, L. *J. Chem. Phys*. **1987**, *87*, 1851–1856.
[16] Born, M.; Wolf, E. *Principles of Optics* (Sixth edition); Pergamon Press: Oxford, 1980.
[17] Galerne, Y.; Marcerou, J.P. *J. Physique* **1985**, *46*, 589–594.
[18] Figueiredo Neto, A.M.; Salinas, S.R. *The Physics of Lyotropic Liquid Crystals*; Oxford University Press: Oxford, New York, 2005.
[19] Galerne, Y.; Marcerou, J.P. *Phys. Rev. Lett*. **1983**, *51*, 2109–2111.
[20] Montecinos, R.; Ahumada, H.; Araya-Maturana, R.; Olea, A.F.; Weiss-Lopez, B.E. *J. Colloid Interface Sci.* **2007**, *316*, 126–131.
[21] Zana, R. *Adv. Colloid Interface Sci*. **1995**, *57*, 1–64.
[22] Hayase, K.; Hayano, S. *Bull. Chem. Soc. Jpn.* **1977**, *50*, 83–85.
[23] Miyashita, Y.; Hayano, S. *J. Colloid Interface Sci.* **1982**, *86*, 344–349.
[24] Hoiland, H.; Ljosland, E.; Backlund, S. *J. Colloid Interface Sci.* **1984**, *101*, 467–471.
[25] Carlfors, J.; Stilbs, P. *J. Colloid Interface Sci.* **1985**, *104*, 489–499.
[26] Treiner, C. *J. Colloid Interface Sci.* **1983**, *93*, 33–42.
[27] Mukerjee, P. *Pure App. Chem*. **1980**, *52*, 1317–1321.
[28] Muto, Y.; Yoda, K.; Yoshida, N.; Esumi, K.; Meguro, K.; Binana-Limbele, W.; Zana, R. *J. Colloid Interface Sci.* **1989**, *130*, 165–175.
[29] Franks, N.P.; Lieb, W.R. *Proc. Natl. Acad. Sci. USA* **1986**, *83*, 5116–5120.
[30] Freiser, M.J. *Phys. Rev. Lett*. **1970**, *24*, 1041–1043.
[31] Shih, C.S.; Alben, R. *J. Chem. Phys*. **1972**, *57*, 3055–3061.
[32] de Gennes, P.G.; Prost, J. *The Physics of Liquid Crystals*; Clarendon Press: Oxford, 1993.
[33] Hendrikx, Y.; Charvolin, J.; Rawiso, M. *Phys. Rev. B: Condens. Matter Mater. Phys.* **1986**, *33*, 3534–3537.
[34] Beaman, D.K.; Robertson, E.J.; Richmond, G.L. *J. Phys. Chem. C* **2011**, *115*, 12508–12516.